

$^{226}\text{Ra}/^{230}\text{Th}$ excess generated in the lower crust: Implications for magma transport and storage time scales

Josef Dufek* } Department of Earth and Space Sciences, Box 351310, University of Washington, Seattle, Washington
Kari M. Cooper* } 98195, USA

ABSTRACT

Excesses of ^{226}Ra in arc magmas have been interpreted as resulting from flux melting of the mantle above subducting slabs, followed by fast ascent rates of magma from slab to surface (up to 1000 m/yr). However, we demonstrate that incongruent melting of the lower crust could either maintain or augment mantle-derived ^{226}Ra excesses, and so reduce inferred vertical transport rates. We developed an incongruent, continuous melting model, and both the incongruent melting reaction and ingrowth effects contribute to the ^{226}Ra excess. In particular, we found that dehydration melting of amphibolite can produce modeled ^{226}Ra excesses greater than 300%. Mixtures of such amphibolite dehydration melts with mantle melts will likely retain a ^{238}U excess (subducted slab) signature. This amphibolite dehydration melting process will also produce elevated ratios of light rare earth elements to heavy rare earth elements, similar to those observed in several arc settings, which may distinguish these magmas from those with ^{226}Ra excesses produced by slab dewatering alone.

Keywords: time scales, melting, ^{226}Ra , ^{238}U , ^{230}Th , lower crust.

INTRODUCTION

Arc magmas have compositions that reflect an integrated history of melt generation processes in the mantle and variable extents of polybaric assimilation and fractionation within the crust. Many continental arc magmas, in particular, have trace-element and isotopic signatures consistent with significant contributions from crustal material (e.g., Davidson et al., 2005). Numerous lines of evidence are consistent with lower crustal assimilation by mantle-derived magmas, including the observation of lower crustal outcrops that preserve evidence of crustal melting (Pickett and Saleeby, 1993; Williams et al., 1995), the trace element signature of residual garnet in some continental arc magmas (Hildreth and Moorbath, 1988), isotopic data consistent with crustal assimilation (Hart et al., 2002), and thermal models that predict enhanced melting in thickened continental crust (Dufek and Bergantz, 2005).

Disequilibria between intermediate daughter products in the decay series of ^{238}U provide a useful chronometer for magmatic processes and ascent rates of magma from depth, sensitive to time scales of ca. 10–350 ka (^{238}U - ^{230}Th disequilibria) or ca. 100 a–10 ka (^{230}Th - ^{226}Ra disequilibria). A combination of (^{238}U)/(^{230}Th) > 1 (^{238}U excess) and (^{226}Ra)/(^{230}Th) > 1 (^{226}Ra excess) is usually observed in arc settings, distinguishing arc lavas from mid-oceanic-ridge basalt (MORB) and oceanic-island basalt (OIB) sources (e.g., Lundstrom, 2003). Typical arc lavas have ^{226}Ra excesses of ~200%–300% [i.e., (^{226}Ra)/

(^{230}Th) = 2–3], although extremely large ^{226}Ra excesses have been observed in a few island arc lavas (>600%; Turner et al., 2000). ^{226}Ra excesses in arc lavas have predominantly been explained by fluid-induced partial melting involving Ra-enriched aqueous fluids deep in the mantle (e.g., Turner et al., 2003). Where interaction of melts with the crust beneath volcanic arcs has been considered, it is assumed to decrease mantle-derived ^{226}Ra excesses due to decay of ^{226}Ra during the time spent in transport and storage. This interpretation implies that the magma has not stalled at any depth for long periods of time relative to the half-life of ^{226}Ra ($t_{1/2} = 1.6$ k.y.).

Other interpretations of ^{226}Ra excesses in arcs are emerging; for example, diffusion-induced disequilibria created in the mantle beneath arcs (Feineman and DePaolo, 2003), or a combination of flux melting and daughter ingrowth during melting (Thomas et al., 2002). However, these mechanisms still focus on processes operating within the mantle, and the degree to which crustal melting and wall-rock interactions can impact U-series disequilibria during storage and ascent of magmas has yet to be fully explored. Recently Berlo et al. (2004) examined the case of batch melting of lower-crustal material at high melt fraction (0.10–0.40) and concluded that U-series activity ratios of these melts were near equilibrium. However, the assumption of congruent batch melting to high melt fraction may be inappropriate under many crustal melting conditions (Rushmer, 1995). For example, mafic, amphibolitic lower crust at pressures of ~10 kbar will undergo incongruent dehydration melting in which amphibole and plagioclase

react to form garnet, pyroxenes, and melt (Wolf and Wyllie, 1994).

We developed an incongruent, continuous melting model for lower crustal conditions (Data Repository¹) to further investigate the role of crustal processes on U-series disequilibria. This model predicts significant ^{226}Ra excesses (>300%), similar to those in the majority of arc lavas, and modest ^{230}Th - ^{238}U disequilibria [(^{230}Th)/(^{238}U) = 0.7–1.12] in melts produced during dehydration melting of the lower crust. When mixed with mantle-derived magmas, the ^{226}Ra excesses generated in melts of deep continental crust may augment pre-existing disequilibria and can relax the ascent time scales inferred for arc magmas.

CONTINUOUS DEHYDRATION MELTING

We extend the work of Zou and Reid (2001) and McKenzie (1985) to incongruent melting with ingrowth of radioactive nuclides. Melt production is modeled as continuous: the melting process occurs at a constant rate in a static (i.e., not upwelling) residue, and the melt fraction below a critical porosity (Φ) is in equilibrium with the residue (Williams and Gill, 1989). Any melt in excess of this critical porosity is instantaneously extracted and aggregated. Ingrowth effects, due to the decay of radioactive nuclides over time, are included in this model. Critical porosity was varied from 10^{-2} to 10^{-1} and is consistent with observations that melt segregation during lower-crustal melting experiments occurs at porosities of a few percent to 15% (Rushmer, 1995). This model is a more physically plausible representation of melting of a static lower crust that is being fluxed with mafic intrusions than is dynamic (i.e., upwelling residue), batch, or fractional melting. The full derivation of the incongruent continuous melting model for both stable elements and radioactive nuclides is included in the Data Repository (see footnote 1). Note that if we apply bulk partition coefficients and melting conditions appropriate for mantle melting to this model, we recover the results of mantle melting calculations (e.g., Zou and Zindler, 2000).

We applied this model to lower-crustal

¹GSA Data Repository item 2005164, Incongruent melting model derivation, is available online at <http://www.geosociety.org/pubs/ft2005.htm>, or on request from editing@geosociety.org or Documents Secretary, GSA, P.O. Box 9140, Boulder, CO 80301-9140, USA.

*E-mails: dufek@u.washington.edu, kmcooper@u.washington.edu

TABLE 1. PARTITION COEFFICIENTS

| | Amp [†] | Plag [§] | Opx [#] | Cpx [*] | Gt ^{††} |
|------------------|----------------------|-------------------|----------------------|----------------------|----------------------|
| Ba | 0.12 | 0.056 | 7.4×10^{-4} | 9.6×10^{-3} | 1.0×10^{-5} |
| Ra ^{**} | 9.6×10^{-3} | 0.008 | 7.4×10^{-6} | 9.6×10^{-5} | 1.0×10^{-9} |
| Th | 0.017 | 0.003 | 0.021 | 0.82 | 0.10 |
| U | 0.008 | 0.0006 | 0.018 | 0.77 | 0.37 |
| Nb | 0.19 | 0.12 | 0.001 | 0.017 | 0.005 |
| La | 0.12 | 0.12 | 0.001 | 0.017 | 0.025 |
| Ce | 0.24 | 0.07 | 0.12 | 0.13 | 0.04 |
| Sr | 0.28 | 1.1 | 0.07 | 0.09 | 0.20 |
| Nd | 0.62 | 0.08 | 0.27 | 0.31 | 0.09 |
| Sm | 1.4 | 0.05 | 0.46 | 0.60 | 0.83 |
| Zr | 0.23 | 0.0001 | 0.027 | 0.23 | 0.52 |
| Eu | 1.1 | 0.07 | 0.35 | 0.69 | 0.74 |
| Ti | 2.0 | 0.02 | 0.24 | 1.3 | 0.79 |
| Gd | 1.5 | 0.03 | 0.01 | 0.82 | 1.1 |
| Dy | 1.8 | 0.02 | 0.02 | 0.99 | 4.4 |
| Y | 1.7 | 0.012 | 0.09 | 1.2 | 10.0 |
| Er | 1.5 | 0.02 | 0.1 | 1.1 | 9.4 |
| Yb | 1.2 | 0.004 | 0.17 | 0.84 | 14.0 |
| Lu | 1.1 | 0.009 | 0.18 | 0.92 | 16.0 |

^{*}(Barth et al., 2002; Klein et al., 2000).

[†](Brenan et al., 1995; Klein et al., 1997).

[§](Bindeman and Davis 2000; Bindeman et al., 1998; Blundy and Wood, 2003).

[#](Beattie, 1993a; McDade et al., 2003).

^{**}Ra partition coeff. calc. with Ba partition coeff. using Blundy and Wood model (2003).

^{††}(Barth et al., 2002; Beattie, 1993b; Klein et al., 2000; van Westrenen et al., 2001).

melting using the specific phase proportions and compositions from the 10 kbar amphibolite dehydration melting experiments of Wolf and Wyllie (1994), appropriate for melting occurring at the base of ~30-km-thick crust. The general form of the incongruent melting reaction is Amp + Plag → Opx + Cpx + Gt + Melt. We used partition coefficients (Ds) relevant to the phases, pressures, and compositions in the lower crust (Table 1), and we assess the sensitivity of the U-series disequilibria to changing anorthite content.

MODEL RESULTS

As incongruent melting proceeds, the production of phases in which radium is highly incompatible (garnet and pyroxene) combined

with the consumption of phases in which Ra is only moderately incompatible (plagioclase and amphibole) act in concert to elevate $(^{226}\text{Ra})/(^{230}\text{Th})$ in the melt well beyond what would be predicted based on congruent melting models (Fig. 1). A further increase over batch melting occurs due to ingrowth of ^{226}Ra in the residual solid during the melting process, and partitioning of Ra into the liquid as melting proceeds. At high melting rates ($>1 \text{ kg/m}^3\text{yr}$) and low critical mass porosity (<0.01), the model disequilibria are comparable to or higher than those produced during congruent batch melting with similar residual mineralogy (cf., Berlo et al., 2004). At slower

melting rates (approaching $\sim 1.0 \times 10^{-4} \text{ kg/m}^3\text{yr}$) the degree of disequilibrium becomes a weak function of melting rate and—as with dynamic melting calculations applied to mantle upwelling— $(^{226}\text{Ra})/(^{230}\text{Th})$ is principally determined by the critical mass porosity, with ratios >5 produced at melting rates of $1.0 \times 10^{-4} \text{ kg/m}^3\text{yr}$ and critical mass porosities of 0.01. At low melting rates, $(^{226}\text{Ra})/(^{230}\text{Th})$ increases as the reaction proceeds due to the combined effect of ^{226}Ra ingrowth and the fact that radium becomes more incompatible in the residue relative to thorium, although the individual activities both decrease with increasing melt fraction. Mixtures of mantle-derived magmas with lower-crustal melts can thus have substantial ^{226}Ra excesses, even if transport times through the mantle wedge were significant.

Both uranium and thorium become less incompatible as the dehydration reaction progresses, and the critical porosity has a modest control on the degree of ^{230}Th - ^{238}U disequilibria. At small critical porosities (<0.01) and low extracted melt fractions (<0.02), $(^{230}\text{Th})/(^{238}\text{U}) = \sim 0.75$. As the dehydration reaction proceeds, the amount of residual garnet increases and uranium becomes increasingly more compatible in the residue. This, combined with ingrowth of ^{230}Th during melting, drives $(^{230}\text{Th})/(^{238}\text{U})$ toward higher values, and ^{230}Th excesses ($\sim 12\%$) develop at high critical porosities and extracted melt fractions greater than 0.2. Considering these modest disequilibria in crustal melts, mixtures of crustal melts with mantle-derived melts will likely be weighted toward ^{238}U excesses, unless extracted melt fractions are high.

Our model also predicts an enrichment of light rare earth elements relative to heavy rare

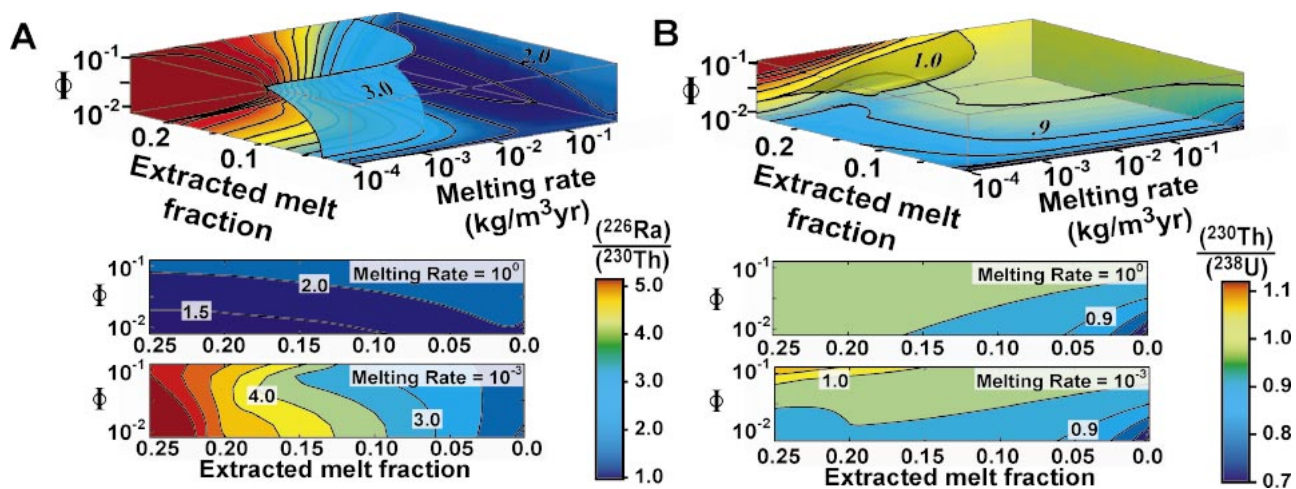
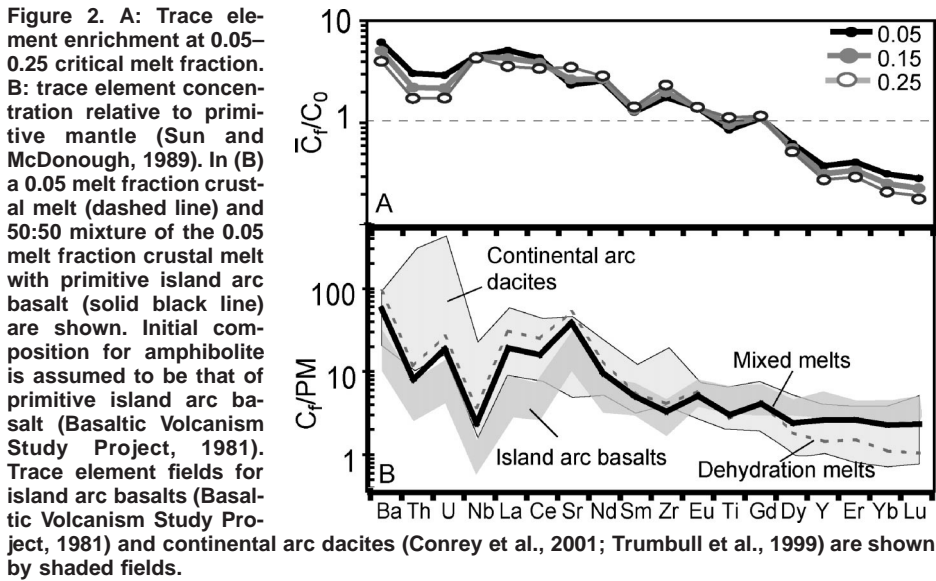


Figure 1. Isosurfaces of (A) $(^{226}\text{Ra})/(^{230}\text{Th})$ and (B) $(^{230}\text{Th})/(^{238}\text{U})$ in the aggregate melt from continuous melting of amphibolite (initial mode: 67% amphibole, 33% plagioclase). Activity ratios are shown for a range of critical mass porosity (Φ), extracted melt fraction, and melting rate. Slices at constant melting rate (0 and $10^{-3} \text{ kg/m}^3\text{yr}$), are also shown. Extracted melt fraction is related to total melt fraction as $F = \Phi + (1 - \Phi)X$, where F is total melt fraction and X is extracted melt fraction. At $F \sim 0.23$, amphibole and plagioclase are consumed and melting reaction becomes congruent melting of the residue resulting in a change in curvature on these plots (Data Repository; see footnote 1).



earth elements in the melt, due in large part to the formation of garnet, as well as enrichment of barium and strontium in the melt due to the melting of plagioclase. Amphibolites present in the lower crust are likely to have formed by stalling and solidification of earlier intrusions of mantle-derived hydrous basalts. We use primitive island arc basalts as a model source composition (Fig. 2B), although the general trace-element behavior (Fig. 2A) will remain the same for a reasonable range of compositions of amphibolite. The trace element pattern follows the same general trend as many continental andesites and dacites (Fig. 2B). When mixed with mantle-derived magmas, amphibolite melts will dominate the trace-element budget of mixtures even when they represent a small mass fraction (see Fig. 2B). Some upper crustal fractionation (involving plagioclase) of amphibolite-derived and/or mixed melts would be required to account for the negative Eu anomalies observed in many continental arc magmas.

Any mixing model must also satisfy major

element constraints. Melts from amphibolite dehydration are andesitic to rhyodacitic. Melts of quartz amphibolites would have the highest SiO₂ concentration (Patiño-Douce and Beard, 1994), whereas amphibolites with more primitive compositions produce melts that (at melt fractions less than 0.2) have 60–64 wt% SiO₂. Mixtures of these crustal melts with mantle-derived basalts will produce intermediate magmas of basaltic andesite to andesite composition.

DISCUSSION

Based on our model results, crustal processes need not act solely to decrease mantle-derived ²²⁶Ra excesses, and U-series disequilibria measured in arc lavas may reflect the influence of multiple processes (Fig. 3). In particular, mixtures of mantle-derived basalt with amphibolite melts can have significant ²²⁶Ra excesses, and trace-element patterns similar to those observed in arc lavas.

There are appreciable uncertainties in the melting rate appropriate for the lower crust;

numerical models of crustal melting predict that melting rates can vary locally from 1.0 to 1.0 × 10⁻⁴ kg/m³yr depending on the flux of basaltic magma and style of intrusion in the crust (Annen and Sparks, 2002; Dufek and Bergantz, 2005) [cf., mantle decompression melting rates of 10⁻³ to 10⁻⁵ kg/m³yr (Bourdon and Sims, 2003)]. However, even assuming instantaneous melting, significant Ra excesses can develop during incongruent melting.

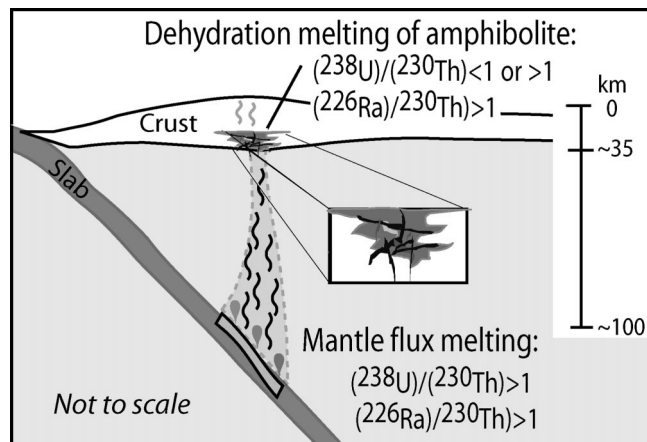
Due to crystal-chemical effects on partitioning, melting of anorthitic plagioclase [e.g., in the Wolf and Wyllie (1994) experiments] produces larger Ra excesses than melting of low-An plagioclase. Aggregate fractional melting of amphibolite with An₅₀ plagioclase produces (²²⁶Ra)/(²³⁰Th) of 1.21–1.55 for the melting range of 0–0.15 melt fraction, similar to the modest excesses predicted by Berlo et al. (2004). However, if melt extraction rates are less than ~10⁻² kg/m³ yr, ingrowth effects will result in Ra excesses exceeding 2.0 at melt fractions of 0.15 even with these lower-An plagioclase compositions.

Stable element patterns can be used to constrain the overall degree of melting for the model. As an example, the La/Yb for lavas from Mount St. Helens are consistent with modeled melt fractions of ~5%–10% (with Φ = 0.1), which yields initial (²²⁶Ra)/(²³⁰Th) excesses of 3.0–4.0 if melting is slow enough for ingrowth effects to develop. Age-corrected (²²⁶Ra)/(²³⁰Th) in recent lavas from Mount St. Helens are 1.46–1.9, and the time to reach (²²⁶Ra)/(²³⁰Th) = 1.5 from an initial disequilibrium of 3.0–4.0 is ~3–4 ky, similar to plagioclase ages in these lavas (Cooper and Reid, 2003). Assuming a crustal thickness of 35 km, this would imply average crustal ascent rates of ~8–10 m/yr, compared to ascent rates exceeding an order of magnitude greater if the disequilibria were generated entirely in the mantle (cf. Turner et al., 2001). Moreover, since the modeled ²²⁶Ra-²³⁰Th disequilibrium is generated as a result of melting processes in the lower crust, it is insensitive to the time spent traversing the mantle wedge. Therefore, the ²²⁶Ra excesses of arc magmas could potentially be decoupled in time from stable trace-element or long-lived isotopic signatures of slab fluids that are carried by older mantle-derived magmas that formed lower-crustal amphibolites.

CONCLUSIONS

Radium excesses observed in island arcs and continental arcs need not be produced exclusively as a result of slab dewatering and resulting flux melting. The exposed roots of arcs show ample evidence for garnet amphibolite compositions that are capable of melting to produce magmas with significant ²²⁶Ra excesses and with either ²³⁰Th or ²³⁸U excesses.

Figure 3. Conceptual model of U-series disequilibria produced by different arc processes. Slab dehydration releases fluids enriched in uranium and radium relative to thorium. These fluids initiate flux melting in the mantle. Melts that reach crustal levels can potentially stall and solidify (producing amphibolite or pyroxenite lithologies), and/or initiate heating and remelting of previous mafic intrusions (amphibolite dehydration), producing melts with ²²⁶Ra excesses and either ²³⁸U excesses or ²³⁰Th excesses.



Mixtures of mantle and crustal melts in the lower crust will most likely be weighted toward ^{238}U excesses. These mixed magmas can have significant ^{226}Ra excesses regardless of the transit time through the mantle wedge, and therefore extreme transport rates in arcs are required only in the case of primitive arc basalts where $(^{226}\text{Ra})/(^{230}\text{Th})$ in arc lavas exceeds 3–5.

ACKNOWLEDGMENTS

This study was supported in part by a National Aeronautics and Space Administration (NASA) Earth Systems Science Fellowship (Dufek) and by EAR-0307691 (Cooper). Discussions and suggestions from G.W. Bergantz and O. Bachmann greatly improved the manuscript. We thank J. Miller, C. Lundstrom, J. Davidson, M. Williams, and an anonymous reviewer for their insightful reviews.

REFERENCES CITED

- Annen, C., and Sparks, R.S.J., 2002, Effects of repetitive emplacement of basaltic intrusions on the thermal evolution and melt generation in the crust: *Earth and Planetary Science Letters*, v. 203, p. 937–955.
- Barth, M.G., Foley, S.F., and Horn, I., 2002, Partial melting in Archean subduction zones: Constraints from experimentally determined trace element partition coefficients between eclogitic minerals and tonalitic melts under upper mantle conditions: *Precambrian Research*, v. 113, p. 323–340.
- Basaltic Volcanism Study Project, 1981, *Basaltic Volcanism of the Terrestrial Planets*: New York, Pergamon Press, Inc., 1286 p.
- Beattie, P., 1993a, The generation of uranium series disequilibria by partial melting of spinel peridotite: Constraints from partitioning studies: *Earth and Planetary Science Letters*, v. 117, p. 379–391.
- Beattie, P., 1993b, Uranium-thorium disequilibria and partitioning on melting of garnet peridotite: *Nature*, v. 363, p. 63–65.
- Berlo, K., Turner, S., Blundy, J., and Hawkeswork, C.J., 2004, The extent of U-series disequilibria produced during partial melting of the lower crust with implications for the formation of Mount St. Helens dacites: *Contributions to Mineralogy and Petrology*, v. 148, p. 122–130.
- Bindeman, I.N., and Davis, A.M., 2000, Trace element partitioning between plagioclase and melt; investigation of dopant influence on partition behavior: *Geochimica et Cosmochimica Acta*, v. 64, p. 2863–2878.
- Bindeman, I.N., Davis, A.M., and Drake, M.J., 1998, Ion microprobe study of plagioclase-basalt partitioning experiments at natural concentration levels of trace elements: *Geochimica et Cosmochimica Acta*, v. 62, p. 1175–1193.
- Blundy, J., and Wood, B., 2003, Mineral-melt partitioning of uranium, thorium and their daughters, *in* Bourdon, B., et al., eds., *Uranium-series geochemistry*: Washington, D.C., Mineralogical Society of America and Geochemical Society, v. 52, p. 59–123.
- Bourdon, B., and Sims, K.W.W., 2003, U-series constraints on intraplate basaltic magmatism, *in* Bourdon, B., et al., eds., *Uranium-series geochemistry*: Washington, D.C., Mineralogical Society of America and Geochemical Society v. 52, p. 215–254.
- Brenan, J.M., Shaw, H.F., Ryerson, F.J., and Phinney, D.L., 1995, Experimental determination of trace-element partitioning between pargasite and a synthetic hydrous andesitic melt: *Earth and Planetary Science Letters*, v. 135, p. 1–11.
- Conrey, R.M., Hooper, P.R., Larson, P.B., Chesley, J.T., and Ruiz, J., 2001, Trace element and isotopic evidence for two types of crustal melting beneath a high Cascade volcanic center, Mt. Jefferson, Oregon: *Contributions to Mineralogy and Petrology*, v. 142, p. 261–283.
- Cooper, K.M., and Reid, M.R., 2003, Re-examination of crystal ages in recent Mount St. Helens lavas: Implications for magma reservoir processes: *Earth and Planetary Science Letters*, v. 213, p. 149–167.
- Davidson, J.P., Hora, J.M., Garrison, J.M., and Dungan, M.A., 2005, Crustal forensics in arc magmas: *Journal of Volcanology and Geothermal Research*, v. 140, p. 157–170.
- Dufek, J.D., and Bergantz, G.W., 2005, Lower crustal magma genesis and preservation: A stochastic framework for the evaluation of basalt-crust interaction: *Journal of Petrology*, doi: 10.1093/ptology/egi049 (in press).
- Feineman, M.D. and DePaolo, D.J., 2003, Steady-state Ra-226/Th-230 disequilibrium in mantle minerals: Implications for melt transport rates in island arcs: *Earth and Planetary Science Letters*, v. 215, p. 339–355.
- Hart, G.L., Johnson, C.M., Shirey, S.B., and Clyne, M.A., 2002, Osmium isotope constraints on lower crustal recycling and pluton preservation at Lassen Volcanic Center, CA: *Earth and Planetary Science Letters*, v. 199, p. 269–285.
- Hildreth, W., and Moorbath, S., 1988, Crustal contributions to arc magmatism in the Andes of central Chile: *Contributions to Mineralogy and Petrology*, v. 98, p. 455–489.
- Klein, M., Stosch, H.G., and Seck, H.A., 1997, Partitioning of high field-strength and rare-earth elements between amphibole and quartz-dioritic to tonalitic melts; an experimental study: *Chemical Geology*, v. 138, p. 257–271.
- Klein, M., Stosch, H.G., Seck, H.A., and Shimizu, N., 2000, Experimental partitioning of high field strength and rare earth elements between clinopyroxene and garnet in andesitic to tonalitic systems: *Geochimica et Cosmochimica Acta*, v. 64, p. 99–115.
- Lundstrom, C.C., 2003, Uranium-series disequilibria in mid-ocean ridge basalts: Observations and models of basalt genesis *in* Bourdon, B., et al., eds., *Uranium-series geochemistry*: Washington, D.C., Mineralogical Society of America and Geochemical Society, v. 52, p. 175–214.
- McDade, P., Blundy, J., and Wood, B., 2003, Trace element partitioning of the Tinaquillo Lherzolite solidus at 1.5 GPa: *Physics of the Earth and Planetary Interiors*, v. 139, p. 129–147.
- McKenzie, D., 1985, ^{230}Th - ^{238}U disequilibrium and the melting processes beneath ridge axes: *Earth and Planetary Science Letters*, v. 72, p. 149–157.
- Patiño-Douce, A., and Beard, J., 1994, Dehydration-melting of biotite gneiss and quartz amphibolite from 3 to 15 kbar: *Journal of Petrology*, v. 36, p. 707–738.
- Pickett, D.A., and Saleeby, J.B., 1993, Thermobarometric constraints on the depth of exposure and conditions of plutonism and metamorphism at deep levels of the Sierra-Nevada Batholith, Tehachapi Mountains, California: *Journal of Geophysical Research*, v. 98, p. 609–629.
- Rushmer, T., 1995, An experimental deformation of partially molten amphibolite: Application to low-melt fraction segregation: *Journal of Geophysical Research*, v. 100, p. 15,681–15,695.
- Sims, K.W.W., DePaolo, D.J., Murrell, M.T., Baldrige, W.S., Goldstein, S., Clague, D., and Jull, M., 1999, Porosity of the melting zone and variations in the solid mantle upwelling rate beneath Hawaii: Inferences from ^{238}U - ^{230}Th - ^{226}Ra and ^{235}U - ^{231}Pa disequilibria: *Geochimica et Cosmochimica Acta*, v. 63, p. 4119–4138.
- Sun, S.S., and McDonough, W.F., 1989, Chemical and isotopic systematics of oceanic basalts; implication for mantle composition and processes, *in* Saunders, A.D., and Norry, M.J., eds., *Magmatism in the ocean basins*: Geological Society [London] Special Publication 42, p. 313–345.
- Thomas, R.S., Hirshmann, M.M., Cheng, H., Reagan, M.K., and Edwards, R.L., 2002, (Pa-231/U-235)-(Th-230/U-238) of young mafic volcanic rocks from Nicaragua and Costa Rica and the influence of flux melting on U-series systematics of arc lavas: *Geochimica et Cosmochimica Acta*, v. 66, p. 4287–4309.
- Trumbull, R.B., Wittenbrink, R., Hahne, K., Emmermann, R., Busch, W., Gerstenberger, H., and Siebel, W., 1999, Evidence for late Miocene to recent contamination of arc andesites by crustal melts in the Chilean Andes (25–26 degrees) and its geodynamic implications: *Journal of South American Earth Sciences*, v. 12, p. 135–155.
- Turner, S., Bourdon, B., Hawkeswork, C., and Evans, P., 2000, ^{226}Ra - ^{230}Th evidence for multiple dehydration events, rapid melt ascent and the time scales of differentiation beneath the Tonga-Kermadec island arc: *Earth and Planetary Science Letters*, v. 179, p. 581–593.
- Turner, S., Evans, P., and Hawkesworth, C., 2001, Ultrafast source-to-surface movement of melt at island arcs from ^{226}Ra - ^{230}Th systematics: *Science*, v. 292, p. 1363–1366.
- Turner, S., Bourdon, B., and Gill, J., 2003, Insights into magma genesis at convergent margins from U-series isotopes, *in* Bourdon, B., et al., eds., *Uranium-series geochemistry*: Washington, D.C., Mineralogical Society of America and Geochemical Society, v. 52, p. 255–310.
- van Westrenen, W., Blundy, J.D., and Wood, B.J., 2001, High field strength element/rare earth element fractionation during partial melting in the presence of garnet: Implications for identification of mantle heterogeneities: *Geochemistry, Geophysics, Geosystems*, v. 2, no. 7.
- Williams, R.W. and Gill, J.B., 1989, Effects of partial melting on the uranium decay series. *Geochimica et Cosmochimica Acta*, v. 53, p. 1607–1619.
- Williams, M.L., Hanmer, S., Kopf, C., and Darrach, M., 1995, Syntectonic generation and segregation of tonalitic melts from amphibolite dikes in the lower crust, Striding-Athabasca mylonite zone, northern Saskatchewan: *Journal of Geophysical Research*, v. 100, p. 15,717–15,734.
- Wolf, M.B., and Wyllie, P.J., 1994, Dehydration-melting of amphibolite at 10 kbar: The effects of temperature and time: *Contributions to Mineralogy and Petrology*, v. 115, p. 369–383.
- Zou, H., and Reid, M., 2001, Quantitative modeling of trace element fractionation during incongruent melting: *Geochimica et Cosmochimica Acta*, v. 65, p. 153–162.
- Zou, H., and Zindler, A., 2000, Theoretical studies of ^{238}U - ^{230}Th - ^{226}Ra and ^{235}U - ^{231}Pa disequilibria in young lavas produced by mantle melting: *Geochimica et Cosmochimica Acta*, v. 64, p. 1809–1817.

Manuscript received 15 April 2005

Revised manuscript received 2 July 2005

Manuscript accepted 6 July 2005

Printed in USA